

ChemComm

Accepted Manuscript



This is an *Accepted Manuscript*, which has been through the Royal Society of Chemistry peer review process and has been accepted for publication.

Accepted Manuscripts are published online shortly after acceptance, before technical editing, formatting and proof reading. Using this free service, authors can make their results available to the community, in citable form, before we publish the edited article. We will replace this *Accepted Manuscript* with the edited and formatted *Advance Article* as soon as it is available.

You can find more information about *Accepted Manuscripts* in the [Information for Authors](#).

Please note that technical editing may introduce minor changes to the text and/or graphics, which may alter content. The journal's standard [Terms & Conditions](#) and the [Ethical guidelines](#) still apply. In no event shall the Royal Society of Chemistry be held responsible for any errors or omissions in this *Accepted Manuscript* or any consequences arising from the use of any information it contains.

Spin canting, metamagnetism, and single-chain magnetic behaviour in a cyano-bridged homospin Iron(II) compound†

Cite this: *Chem. Commun.*, 2014, *?*, *?*

Received 00th January 2014,

Accepted 00th January 2014

DOI: 10.1039/x0xx00000x

www.rsc.org/chemcomm

Spin canting, antiferromagnetic ordering, metamagnetism and single-chain magnetism were verified in a cyano-bridged Fe^{II} compound synthesized from the pentagonal bipyramidal Fe^{II} starting material in the presence of excessive BF₄⁻ anion.

Single-chain magnets (SCMs) showing Glauber slow dynamics¹ and a magnetic hysteresis of molecular origin have attracted considerable interest in the field of molecular magnetism.²⁻³ For the rational design of SCMs, strong intrachain magnetic coupling and spin carriers of large magnetic anisotropy (preferably of Ising type) are essential ingredients.⁴ It was also believed that negligible interchain coupling is necessary to prevent the three-dimensional magnetic ordering until the discovery of SCM behaviour in the antiferromagnetic (AF)⁴ and ferromagnetic (F)⁵ ordered phases. By taking advantage of the AF ordering, new types of high temperature SCM-based magnets can be achieved.^{6,7} However, due to the challenge to design and even to control the interchain magnetic coupling, not to mention the difficulty to design the regular SCMs, examples of the SCM-based magnets are rather limited in the literature.⁴⁻⁷

Since AF interaction is much more common and usually stronger than the F coupling, most SCMs are constructed using the ferrimagnetic strategy with hetero-spin centres. The homospin SCMs, with either parallel or canted antiparallel spin arrangement, are quite fewer.^{6c,9,7-9} For those homospin SCMs, the bridges between the spin centres are usually three-atom bridges, such as the phosphonates,^{8a-b} azide,^{6c-d,8c-d} selenocyanate,^{6e,6f} carboxylates,⁹ mixed azide-carboxylates⁷ and so on. Due to its great ability for the magnetic coupling, cyanide group should be very promising for the construction of homospin SCMs.

As for the anisotropic spin carriers, the pentagonal bipyramidal metal centres with pentadentate macrocyclic ligands are very attractive.¹⁰⁻¹³ Besides the fact that they bear large magnetic anisotropy as established by both experimental and theoretical studies,^{10b,10e,13} these systems are excellent building blocks for the preparation of clusters,¹⁰ chains¹¹ and higher dimensional materials¹² due to the axial weakly coordinated solvent molecules. For example, starting from the iron compounds, [Fe(L_{N3O2})]²⁺ and [Fe(L_{N5})]²⁺ (L_{N3O2} = 2,13-dimethyl-6,9-dioxa-3,12,18-triazabicyclo[12.3.1]octadeca-1(18),2,12,14,16-pentaene, L_{N5} = 2,13-dimethyl-3,6,9,12-tetraaza-1(2,6)pyridinacyclotridecaphane-2,12-diene), a Cr^{III}Fe^{II}₂ trinuclear

SMM and a {Nb^{IV}Fe^I}_{2}∞ SCM were prepared from the reaction of the starting materials with the [Cr(CN)₆]³⁻ and [Nb(CN)₈]⁴⁻ groups.^{10a,11b}

Inspired by the aforementioned consideration, we aimed at the construction of functional magnetic materials from the pentagonal bipyramidal metal centres. In this regard, the photoactive spin crossover compound [Fe(L_{N5})(CN)₂] (Fig. 1a) is very promising as the axial CN groups have the great potential to bridge other metal centres while maintaining their photoactive SCO behaviour and high magnetic anisotropy.¹⁴ Photomagnetic systems with higher nuclearity and dimensionality are thus anticipated, as demonstrated well by Sato and Clérac in their photomagnetic 1D compounds.^{11a,c} Surprisingly, we noticed in our study that the [Fe(L_{N5})(CN)₂] motif has limited stability during the reaction. In the presence of excessive BF₄⁻ anion, a cyano-bridged Fe^{II} compound [Fe(L_{N5})(CN)](BF₄) (**1**) with regular chain structure was obtained. This compound shows the coexistence of spin canting, AF ordering, metamagnetism, and SCM behaviour, and represents a rare example of a cyano-bridged homospin SCM.

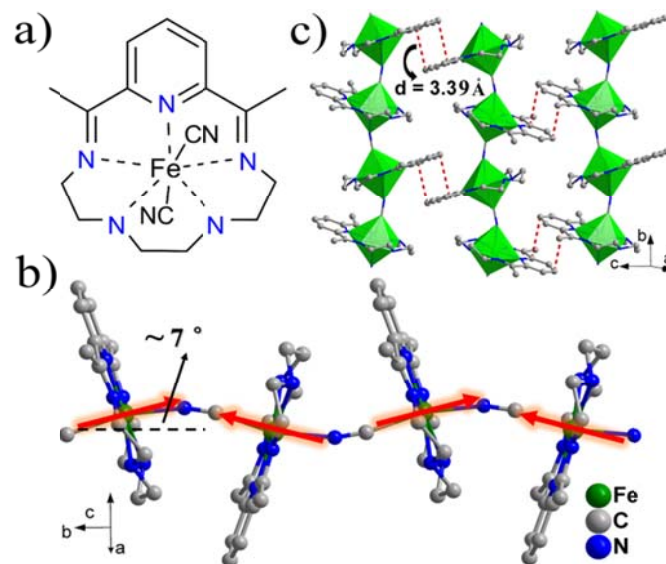


Fig. 1 View of the structure of [Fe(L_{N5})(CN)₂] (a), the cyano-bridged 1D chain structure (b), and the 2D layer structure with π - π interaction (c) of **1**. The arrows represent the axial axis of the Fe^{II} centres, which make an angle of $\sim 7^\circ$ with the *b* axis.

Initially, **1** was obtained by the reaction of $[\text{Fe}(\text{L}_{\text{N}_5})\text{CN}]_2$ with the metal salts like $\text{Fe}(\text{L})(\text{BF}_4)_2$ and $\text{Co}(\text{L})(\text{BF}_4)_2$ (L = other ligands). Then, the reaction was performed by direct addition of excessive simple salt like NaBF_4 to the solution of $[\text{Fe}(\text{L}_{\text{N}_5})\text{CN}]_2$, resulting in a higher yield and purity (see ESI†). With other bulky anions, similar chain compounds of different interchain distances (and magnetic interactions) can be obtained and will be reported later.

X-ray crystallographic analysis revealed that compound **1** crystallizes in the monoclinic space group $P2_1/n$ (Table S1, ESI†) and has a regular chain structure (Fig. 1). In the crystal structure, there is only one unique Fe^{II} center located in the cavity of the L_{N_5} ligand, one unique CN^- group, and one BF_4^- counter anion for charge balance (Fig. S1, ESI†). Coordinated by five equatorial nitrogen atoms from L_{N_5} , one nitrogen atom and one carbon atom from the axial CN^- groups ($\text{Fe}-\text{N}_{\text{cyano}} = 2.199 \text{ \AA}$, $\text{Fe}-\text{C}_{\text{cyano}} = 2.190 \text{ \AA}$), the Fe^{II} centre has a slightly distorted pentagonal bipyramid environment, with a continuous shape measure (CSHM)³⁵ calculated to be 0.406, close to the ideal D_{5h} geometry. Different from the starting material where the coordination sphere of Fe^{II} is N_5C_2 , the rearrangement of the CN^- group results in a N_6C_1 coordination sphere of Fe^{II} , which leads to a weaker ligand field and the high spin state of Fe^{II} in the whole temperature range (vide post). Bridged by the cyano groups, regular chains are formed with the shortest Fe-Fe distance of 5.387 \AA (Fig. 1b). Interestingly, although the 1D chain runs along the b axis, the pseudo 5-fold axis the Fe^{II} center ($\text{C}_{\text{cyano}}-\text{Fe}-\text{N}_{\text{cyano}}$ axis) is tilted away from the b axis with an angle of $\sim 7^\circ$ (Fig. 1b). This canting of the axial axis is important to the magnetic property of **1**, as can be seen below. Linked by the obvious $\pi\cdots\pi$ stacking interactions ($d = 3.39 \text{ \AA}$) between the pyridine rings, these chains form a two-dimensional layer (Fig. 1c), which is further separated by the BF_4^- anions located in between with the shortest interchain Fe \cdots Fe distance of 9.73 \AA (Fig. S2, ESI†).

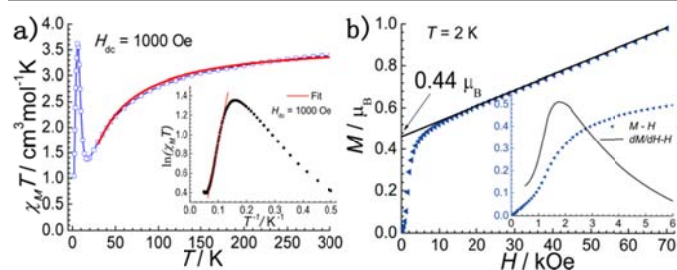


Fig. 2 (a) Dc magnetic susceptibility of **1** measured at 1 kOe. Inset: $\ln(\chi_M T)$ vs. $1/T$ plot. (b) Field dependent magnetization curve at 2 K for **1**. Inset: the $M(H)$ curve and the derivative of the magnetization (dM/dH) at low fields. The field sweep rate is 300 Oe/s.

Direct current (dc) magnetic susceptibility of **1** was measured on polycrystalline samples between 2 to 300 K at 1 kOe (Fig. 2a). At 300 K, the $\chi_M T$ value of **1** is $3.41 \text{ cm}^3 \text{ mol}^{-1} \text{ K}$. This value is larger than the spin-only value of $3.00 \text{ cm}^3 \text{ mol}^{-1} \text{ K}$ for a high-spin Fe^{II} ion ($S = 2$, $g = 2$), reflecting the magnetic anisotropy of Fe^{II} in a nearly D_{5h} ligand field.^{31b,c} Upon cooling, the $\chi_M T$ value decreases to a minimum of $1.37 \text{ cm}^3 \text{ mol}^{-1} \text{ K}$ at 18 K, and then increases sharply to a maximum of $3.61 \text{ cm}^3 \text{ mol}^{-1} \text{ K}$ at 5 K, and finally decreases again down to 2 K. The Curie-Weiss fit of the susceptibility data above 100 K gave the Curie constant $C = 3.80 \text{ cm}^3 \text{ mol}^{-1} \text{ K}$ and the Weiss constant $\vartheta = -37.4 \text{ K}$. To

estimate the intrachain magnetic interaction in **1**, the susceptibility data above 30 K were fitted by the Fisher model ($H = -J \sum_i S_i S_{i+1}$):¹⁶

$$\chi_{\text{chain}} T = \frac{Ng^2 \beta^2 S(S+1)}{3k} \frac{1+u}{1-u}, \text{ where } u = \coth \left[\frac{JS(S+1)}{kT} \right] - \left[\frac{kT}{JS(S+1)} \right].$$

The best fit gave $J = -4.35 (7) \text{ cm}^{-1}$, $g = 2.20 (1)$ ($R = \frac{\sum[(\chi T)_{\text{obsd}} - (\chi T)_{\text{calcd}}]^2}{\sum[(\chi T)_{\text{obsd}}]^2} = 1.0 \times 10^{-3}$), confirming the AF interaction between the Fe^{II} centres through the cyanide group. The $\chi_M T$ curve of **1** is reminiscent of the ferrimagnetic behaviour or the weak ferromagnetism due to spin canting. As there is only one unique Fe^{II} spin in the structure, the sharp increase of the $\chi_M T$ curve below 5 K suggests the occurrence of spin canting.¹⁷ The final decrease of $\chi_M T$ indicates the antiferromagnetic ground state.

The occurrence of the AF ground state and weak ferromagnetism were confirmed by the field dependent magnetization of **1** measured at 2 K. As can be seen in Fig 2b, the $M(H)$ curve has an obvious S-shape curve, typical for a metamagnetic phase transition from an AF state to a state of spontaneous magnetization. As observed in a spin canted weak ferromagnet, when the field is larger than 10 kOe, M increases linearly to the largest value of $0.98 \mu_B$ at 70 kOe, which is far from the saturation value of $4 \mu_B$ for a high spin Fe^{II} with $S = 2$. Extrapolating the $M(H)$ curve in the high field region down to zero gives a small spontaneous magnetization of $0.44 \mu_B$, from which the canting angle is estimated to be 6.3° . This canting angle agrees very well to the included angle (7°) between the axial directions of the Fe^{II} centres and the b axis.

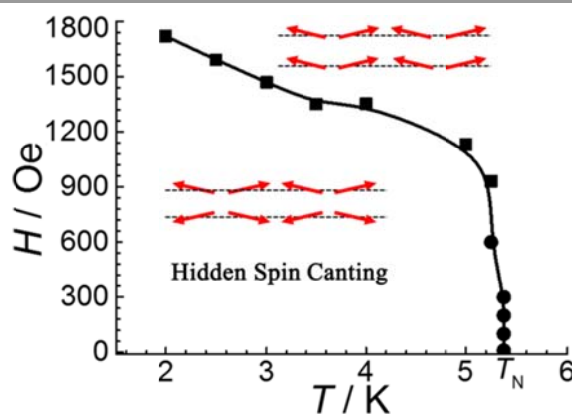


Fig. 3 The H - T magnetic phase diagram of **1**. The squares and circles are from the $M(H)$ and $M(T)$ curves, respectively.

The above observations of **1** can be described as “hidden” spin canting.^{17a} Within the chain, the AF coupled spins are canted to each other resulting in a small, but non-negligible magnetization, which is further coupled to each other by the interchain AF coupling and leads to the AF ground state. Application of an external dc field overcomes the interchain AF coupling and the metamagnetic transition occurs. The critical field H_c for the phase transition at 2 K is deduced to be about 1720 Oe from the peak in the dM/dH curve (Fig. 2b). To obtain the phase diagram of the metamagnetic phase transition, a series of $M(H)$ curves at different temperatures and $\chi_M(T)$ curves at different dc fields were measured (Fig. S3-S5, ESI†). The critical (H , T) values corresponding to the phase boundary in the magnetic phase diagram was thus be obtained. As can be seen from the H - T phase diagram shown in Fig. 3, compound **1** possesses an ordered antiferromagnetic

ground state (hidden spin canting state) below the phase boundary and transfers to a saturated paramagnetic phase at higher temperature and/or a field-polarized weak ferromagnetic state at higher field below T_c .

The magnetic property of **1** was further studied with ac susceptibility measurements below 10 K (Fig. 4). The AF ordering of **1** is confirmed by the frequency-independent peaks at 5.4 K in the χ' curves. Below 5 K, both components of the ac susceptibility exhibit frequency-dependent signals, reflecting the slow magnetic relaxation. The shift of the peak temperature (T_p) of χ'' is measured by the Mydosh parameter $\varphi = (\Delta T_p/T_p)/(\Delta \log f) = 0.16$, which is in the range ($0.1 < \varphi < 0.3$) expected for superparamagnetic behaviour.¹⁸ From the fitting of the relaxation time to the Arrhenius law $\tau = \tau_0 \exp(\Delta_f/T)$, the effective energy barrier Δ_f was estimated to be 35.9 K, with the pre-exponential factor τ_0 being 5.6×10^{-9} s (Fig. S7, ESI[†]). To study the influence of the metamagnetic phase transition on the dynamic behaviour, the ac susceptibilities were measured at a dc field of 2200 Oe (Fig. 4b). As can be seen, the frequency-independent χ' peak at $T_N = 5.4$ K observed under zero dc field disappears, consistent with the metamagnetic phase transition and the fading of AF ordering. Meanwhile, the peaks with frequency dependency don't change much. Analysis on the data gave a slightly larger Δ_f value (39.1 K, Fig. S8, ESI[†]). Furthermore, the Cole-Cole diagrams were also measured under a dc field of 0 and 2200 Oe (Fig. S9-10, ESI[†]) at temperatures from 2.8 to 3.4 K. The semicircles were fitted by the generalized Debye model.¹⁹ The obtained α parameters are 0.13-0.29 ($H_{dc} = 0$ Oe) and 0.21-0.33 ($H_{dc} = 2200$ Oe) (Table S3, ESI[†]), suggesting a moderate distribution of the relaxation time of **1**.²⁰ It seems that the metamagnetic phase transition has a small impact on the magnetic dynamics of the SCM behaviour.

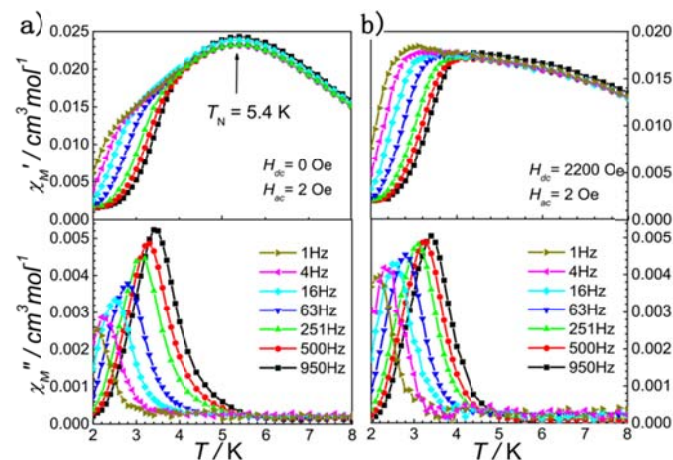


Fig. 4 The real (χ') and imaginary (χ'') parts of the ac susceptibilities for **1** in zero (a) and 2200 Oe dc field (b).

To further investigate the one-dimensional Ising character of the compound, the $\ln(\chi_M T)$ versus $1/T$ plot was plotted (Fig. 2a). As can be seen, a linear regime is observed from 8 to 16 K, indicating an exponential dependence of the Ising-like intrachain correlation length.^{3a} A linear fitting of the data using the expression $\chi T = C_{\text{eff}} \exp(\Delta_f/T)$ leads to $C_{\text{eff}} = 0.66 \text{ cm}^3 \text{ mol}^{-1} \text{ K}$ and $\Delta_f = 15.8 \text{ K}$, respectively. The activation energy Δ_f gives an estimation of the intrachain exchange energy cost to create a domain wall along the

chain. The energy barrier Δ_f is significantly smaller than Δ_f extracted from the ac susceptibility data, suggesting that the relaxation mechanism in **1** cannot be described by a simple Glauber model.^{3a,3e} For an Ising-like SCM, the energy barrier for the spin reversal Δ_f is $\Delta_f = 2\Delta_f + \Delta_A$ for the "infinite chain" at high temperature and $\Delta_f = \Delta_f + \Delta_A$ for the "finite-size chain" at low temperature, where Δ_A represents the intrinsic anisotropic barrier for the individual spin in the absence of magnetic exchange.^{3d} As the relaxation time of **1** was determined below 4 K in the "finite-size chain" regime, we can estimate the anisotropy barrier for the individual Fe^{2+} centres to be $\Delta_A = \Delta_f - \Delta_f = 20.1 \text{ K}$. In addition, for a normal SCM without any long-range ordering, the χT product usually saturates at low temperatures due to finite size effects.^{3a,21} However for **1**, the obvious decrease is observed at zero field, consistent with the AF ordering as observed in several other SCM-based antiferromagnets.^{4,6-7}

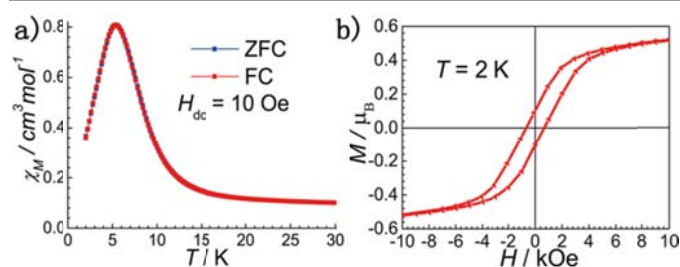


Fig. 5 (a) ZFC/FC curves for compound **1** at $H_{dc} = 10$ Oe; (b) Hysteresis loop of **1** measured at 2 K with the field sweep rate of 500 Oe/s.

Finally, the zero-field-cooled (ZFC) and field-cooled (FC) magnetization at 10 Oe and hysteresis loop at 2.0 K (where the relaxation time is estimated to be 0.35 s) were measured to probe the hysteretic behaviour of **1**. As can be seen from Fig. 5a, both the ZFC and FC curves coincide with each other and show a very sharp peak at 5.4 K. This is consistent with the AF ground state and means that the relaxation is very fast compared to the timescale of the ZFC/FC measurements. However, obvious hysteresis loop with a coercive field of 680 Oe can be observed indeed with a fast field sweep rate of 500 Oe/s (Fig. 5b). The observation of the hysteresis loops in the SCM-based antiferromagnets has been reported in several other compounds.^{4, 6a, 6e-6f, 7a} Although some other factors might complicate the hysteresis loops,^{6f} the slow magnetic relaxation of the SCM behaviour should be the main reason for this observation.

Conclusions

In conclusion, we reported a cyano-bridged Fe^{II} compound synthesized from the anisotropic pentagonal bipyramidal Fe^{II} starting material in the presence of excessive BF_4^- anion. This compound represents a rare example of a cyano-bridged homospin system with the single-chain magnet dynamics. Detailed magnetic measurements revealed that this compound exhibits the rare coexistence of spin-canting, antiferromagnetic ordering, field-induced metamagnetism and single-chain magnet behaviour. Further efforts will be aimed at materials with anions of different size and functionality, such as chirality and so on, to finely tune the interchain magnetic interactions and also the physical properties of the materials.

We thank the Major State Basic Research Development Program (2013CB922102), NSFC (91022034, 21101093, 21471077). This work was also supported by a Project Funded by the Priority Academic Program Development of Jiangsu Higher Education Institutions.

Notes and references

State Key Laboratory of Coordination Chemistry, Collaborative Innovation Center of Advanced Microstructures, School of Chemistry and Chemical Engineering, Nanjing University, Nanjing, 210093, China. Fax: +86-25-83314502. E-mail: wangxy66@nju.edu.cn

† Electronic supplementary information (ESI) available: Experimental section, structure information in detail and additional magnetic data. For ESI and crystallographic data in CIFs or other electronic format see DOI: 10.1039/c000000x/

- 1 (a) R. J. Glauber, *J. Math. Phys.* 1963, **4**, 294.
- 2 (a) A. Caneschi, D. Gatteschi, N. Lalioti, C. Sangregorio, R. Sessoli, G. Venturi, A. Vindigni, A. Rettori, M. G. Pini and M. A. Novak, *Angew. Chem., Int. Ed.*, 2001, **40**, 1760; (b) R. Clérac, H. Miyasaka, M. Yamashita and C. Coulon, *J. Am. Chem. Soc.*, 2002, **124**, 12837.
- 3 (a) C. Coulon, H. Miyasaka and R. Clerac, *Struct. Bonding*, 2006, **122**, 163; (b) L. Bogani, A. Vindigni, R. Sessoli and D. Gatteschi, *J. Mater. Chem.*, 2008, **18**, 4750; (c) H. Miyasaka, M. Julve, M. Yamashita and R. Clérac, *Inorg. Chem.*, 2009, **48**, 3420; (d) H.-L. Sun, Z.-M. Wang and S. Gao, *Coord. Chem. Rev.*, 2010, **254**, 1081; (e) W.-X. Zhang, R. Ishikawa, B. Breedlove and M. Yamashita, *RSC Advances*, 2013, **3**, 3772.
- 4 C. Coulon, R. Clérac, W. Wernsdorfer, T. Colin and H. Miyasaka, *Phys. Rev. Lett.*, 2009, **102**, 167204.
- 5 (a) N. Ishii, Y. Okamura, S. Chiba, T. Nogami and T. Ishida, *J. Am. Chem. Soc.*, 2008, **130**, 24; (b) R. Sessoli, *Angew. Chem., Int. Ed.*, 2008, **47**, 5508.
- 6 (a) H. Miyasaka, K. Takayama, A. Saitoh, S. Furukawa, M. Yamashita and R. Clérac, *Chem. -Eur. J.*, 2010, **16**, 3656; (b) T. Liu, Y.-J. Zhang, S. Kanegawa and O. Sato, *J. Am. Chem. Soc.*, 2010, **132**, 8250; (c) J. H. Yoon, J. W. Lee, D. W. Ryu, S. W. Yoon, B. J. Suh, H. C. Kim and C. S. Hong, *Chem. -Eur. J.*, 2011, **17**, 3028; (d) C.-I. Yang, P.-H. Chuang and K.-L. Lu, *Chem. Commun.*, 2011, **47**, 4445; (e) J. Boeckmann, M. Wriedt and C. Näther, *Chem. -Eur. J.*, 2012, **18**, 5284; (f) S. Wöhlert, T. Fic, Z. Tomkowicz, S. G. Ebbinghaus, M. Rams, W. Haase, C. Näther, *Inorg. Chem.*, 2013, **52**, 12947; (g) L. Qin, Z. Zhang, Z.-P. Zheng, M. Speldrich, P. Kögerler, W. Xue, B.-Y. Wang, X.-M. Chen and Y.-Z. Zheng, *Dalton Trans.*, 2015, **44**, 1456; (h) Y.-Q. Wang, Q. Yue, Y. Qi, K. Wang, Q. Sun and E.-Q. Gao, *Inorg. Chem.*, 2013, **52**, 4259.
- 7 (a) X.-M. Zhang, Y.-Q. Wang, K. Wang, E.-Q. Gao and C.-M. Liu, *Chem. Commun.*, 2011, **47**, 1814; (b) X.-M. Zhang, K. Wang, Y.-Q. Wang and E.-Q. Gao, *Dalton Trans.*, 2011, **40**, 12742; (c) Q.-X. Jia, H. Tian, J.-Y. Zhang and E.-Q. Gao, *Chem. -Eur. J.*, 2011, **17**, 1040; (d) Y.-Q. Wang, W.-W. Sun, Z.-D. Wang, Q.-X. Jia, E.-Q. Gao and Y. Song, *Chem. Commun.*, 2011, **47**, 6386; (e) X.-B. Li, J.-Y. Zhang, Y.-Q. Wang, Y. Song and E.-Q. Gao, *Chem. -Eur. J.*, 2011, **17**, 13883; (f) X.-B. Li, G.-M. Zhuang, X. Wang, K. Wang and E.-Q. Gao, *Chem. Commun.*, 2013, **49**, 1814.
- 8 (a) K. Bernot, J. Luzon, R. Sessoli, A. Vindigni, J. Thion, S. Richeter, D. Leclercq, J. Larionova and A. D. Lee, *J. Am. Chem. Soc.*, 2002, **130**, 1619; (b) Z.-M. Sun, A. V. Prosvirin, H.-H. Zhao, J.-G. Mao and K. R. Dunbar, *J. Appl. Phys.*, 2005, **97**, 10B305; (c) T.-F. Liu, D. Fu, S. Gao, Y.-Z. Zhang, H.-L. Sun, G. Su and Y.-J. Liu, *J. Am. Chem. Soc.*, 2003, **125**, 13976; (d) Z.-X. Li, Y.-F. Zeng, H. Ma and X.-H. Bu, *Chem. Commun.*, 2010, **46**, 8540.
- 9 (a) Y.-Z. Zheng, M.-L. Tong, W.-X. Zhang and X.-M. Chen, *Angew. Chem., Int. Ed.*, 2006, **45**, 6310; (b) S. W. Przybylak, F. Tuna, S. J. Teat and R. E. P. Winpenny, *Chem. Commun.*, 2008, **17**, 1983; (c) S.-Y. Zhang, W. Shi, Y.-H. Lan, N. Xu, X.-Q. Zhao, A. K. Powell, B. Zhao, P. Cheng, D.-Z. Liao and S.-P. Yan, *Chem. Commun.*, 2011, **47**, 2859; (d) J.-P. Zhao, Q. Yang, Z.-Y. Liu, R. Zhao, B.-W. Hu, M. Du, Z. Chang and X.-H. Bu, *Chem. Commun.*, 2012, **48**, 6568; (e) W.-X. Zhang, T. Shiga, H. Miyasaka and M. Yamashita, *J. Am. Chem. Soc.*, 2012, **134**, 6908; (f) J.-Y. Zou, W. Shi, N. Xu, L.-L. Li, J.-K. Tang, H.-L. Gao, J.-Z. Cui and P. Cheng, *Chem. Commun.*, 2013, **49**, 8226.
- 10 (a) Y.-Z. Zhang, B.-W. Wang, O. Sato and S. Gao, *Chem. Commun.*, 2010, **46**, 6959; (b) L. J. Batchelor, M. Sangalli, R. Guillot, N. Guihéry, R. Maurice, F. Tuna and T. Mallah, *Inorg. Chem.*, 2011, **50**, 12045; (c) R. Ruamps, L. J. Batchelor, R. Maurice, N. Gogoi, J. L. Pablo, N. Guihry, C. Graaf, A. L. Barra, J. P. Sutter and T. Mallah, *Chem. -Eur. J.*, 2013, **19**, 950; (d) N. Gogoi, M. Thlijeni, C. Duhayon and J. P. Sutter, *Inorg. Chem.*, 2013, **52**, 2283; (e) X.-C. Huang, C. Zhou, D. Shao and X.-Y. Wang, *Inorg. Chem.*, DOI: 10.1021/ic502006s.
- 11 (a) S. Hayami, G. Juhasz, Y. Maeda, T. Yokoyama and O. Sato, *Inorg. Chem.*, 2005, **44**, 7289; (b) T. S. Venkatakrisnan, S. Sahoo, N. Bréfuel, C. Paulsen, C. Duhayon, A. L. Barra, S. Ramasesha and J. P. Sutter, *J. Am. Chem. Soc.*, 2010, **132**, 6047; (c) R. Ababei, C. Pichon, O. Roubeau, Y.-G. Li, N. Bréfuel, L. Buisson, P. Guionneau, C. Mathonière and R. Clérac, *J. Am. Chem. Soc.*, 2013, **135**, 14840.
- 12 (a) Y.-Z. Zhang, O. Sato, *Inorg. Chem.*, 2010, **49**, 1271; (b) A. Dogaru, C. Pichon, R. Ababei, D. Mitcov, C. Maxim, L. Toupet, C. Mathoniere, R. Clérac and M. Andruh, *Polyhedron*, 2014, **75**, 146.
- 13 R. Ruamps, L. J. Batchelor, R. Maurice, N. Gogoi, P. Jiménez-Lozano, N. Guihéry, C. Graaf, A. L. Barra, J.-P. Sutter and Mallah, *T. Chem. -Eur. J.*, 2013, **19**, 950.
- 14 J. S. Costa, C. Balde, C. Carbonera, D. Denux, A. Wattiaux, C. Desplanches, J. P. Ader, P. Gutlich and J. F. Létard, *Inorg. Chem.*, 2007, **46**, 4114.
- 15 M. Llunell, D. Casanova, J. Cirera, P. Alemany and S. Alvarez, SHAPE, Version 2.1. Universitat de Barcelona, 2013.
- 16 O. Kahn, *Molecular Magnetism*, Wiley-VCH, 1993, chapter 11, p. 258.
- 17 (a) X.-Y. Wang, L. Wang, Z.-M. Wang, G. Su and S. Gao, *Chem. Mater.* 2005, **17**, 6369; (b) X.-Y. Wang, L. Wang, Z.-M. Wang and S. Gao, *Inorg. Chem.*, 2008, **47**, 5720.
- 18 J. A. Mydosh, *Spin Glasses : An Experimental Introduction*, Taylor & Francis, London, 1993.
- 19 K. S. Cole and R. H. Cole, *J. Chem. Phys.*, 1941, **9**, 341.
- 20 S. M. J. Aubin, Z. Sun, L. Pardi, J. Krzystek, K. Folting, L. C. Brunel, A. L. Rheingold, G. Christou, D. N. Hendrickson, *Inorg. Chem.*, 1999, **38**, 5329.
- 21 C. Coulon, R. Clérac, L. Lecren, W. Wernsdorfer and H. Miyasaka, *Phys. Rev. B*, 2004, **69**, 132408.